

FINAL REPORT

Spatial Map for Thermal Image Processing at Wendelstein 7-X

A Degree Thesis
Submitted to the Faculty of the
Escola Tècnica d'Enginyeria de Telecomunicació de Barcelona
Universitat Politècnica de Catalunya

by
Kim Jung, Jae Hyouk

Advisor:
Casas Pla, Josep R.

Barcelona, July 2021

Abstract

Wendelstein 7-X is a Stellarator fusion reactor prototype. Many experiments are currently being performed obtaining data from cameras located at different points of the reactor.

In this project, image processing is applied to treat these data in order to analyze the behavior of the plasma and the temperature at each instant. Using the captured images, we study the physical reactor surface covered by every pixel so as to achieve which elements are overheating or to detect anomalies.

Resum

Wendelstein 7-X és un prototip de reactor de fusió Stellarator. Actualment es realitzen experiments en els quals s'obtenen moltes dades a partir de càmeres situades a diferents punts del reactor.

En aquest projecte es tracten aquestes dades aplicant coneixements de processament d'imatge per tal d'obtenir característiques que serveixin per analitzar el comportament del plasma i la temperatura en cada instant. D'aquesta manera, utilitzant les imatges capturades, es calcula quina superfície física del reactor és visualitzada pel camp visual de cada píxel i així poder saber quins elements del reactor s'estan tractant per veure en el futur si s'estan sobreescalfant o poder estudiar altres tipus de comportament.

Resumen

Wendelstein 7-X es un prototipo de reactor de fusión Stellarator. Actualmente se realizan experimentos en los que se obtienen datos a partir de cámaras situadas en diferentes puntos del reactor.

En este proyecto se tratan estos datos aplicando conocimientos de procesamiento de imagen para obtener características que sirvan para analizar el comportamiento del plasma y la temperatura en cada instante. Utilizando las imágenes capturadas, se estudia cuál es la superficie física del reactor cubierta por el campo visual de cada pixel. De esta manera se puede saber qué elementos se están tratando para en un futuro saber si se están sobrecalentando o poder estudiar otro tipo de comportamientos.

Acknowledgements

First, I want to thank my tutor Josep Ramon Casas for giving me the opportunity to be part of this project and the support and motivation he has given me in all aspects. I want to express my gratitude to Mireia for the immense patience she had with me, listening and supporting me being at my side whenever I needed it.

On the other hand, I want to acknowledge professor Josep Pegueroles for the help he gave me with all the problems I had and I want to express my gratitude to my friends Mambos to support me, specially Edu Salgado.

Finally, I want to thank my parents and my sister for all the dedication and effort they have had with me to bring me here and for being by my side supporting me in difficult times.

Revision history and approval record

Revision	Date	Purpose
0	01/07/2021	Document creation
1	06/07/2021	Document revision

DOCUMENT DISTRIBUTION LIST

Name	e-mail
Jae Hyouk Kim Jung	alexkimbcn@gmail.com
Josep Ramon Casas Pla	josep.ramon.casas@upc.edu

Written by:		Reviewed and approved by:	
Date	25/06/2021	Date	01/07/2021
Name	Jae Hyouk Kim Jung	Name	Josep Ramon Casas Pla
Position	Project Author	Position	Project Supervisor

Table of contents

1	Introduction	8
1.1	Statement of purpose	8
1.2	Requirements and specifications	8
1.3	Methods and procedures	9
1.4	Work Plan	10
1.4.1	Work Packages	10
1.4.2	Gantt Diagram	10
2	Background	11
2.1	Introduction to nuclear fusion	11
2.2	Wendelstein 7-x	12
2.2.1	Introduction to W7-X	12
2.2.2	Structure of the reactor	12
2.2.3	Infrared cameras	13
2.2.4	Images in the infrared spectrum	14
3	Methodology	15
3.1	Scene model attributes (CAD) stored in the experimental file format (.h5) used for W7-X	15
3.1.1	HDF5 format	15
3.1.2	Spatial Map	15
3.1.3	Scene model	16
3.2	Geometric strategy to estimate the surface of the corresponding element being projected for each IR image pixel	17
3.3	Software development to obtain the surface estimation	21
3.4	Method to validate the estimation and error evaluation	22
4	Results and statistics	23
4.1	Estimation of the surface of the corresponding element being projected for each IR image pixel	23
4.2	Results	25
4.3	Project real application	32
5	Conclusions and Further Research	35
6	Bibliography	36

1 Introduction

1.1 Statement of purpose

This project is part of a collaboration between Image Processing Group (GPI) in Barcelona, Institute of Plasma Physics (IPP) of Greifswald (Germany) and the EUROfusion group.

During the last years, several collaborative projects have been carried out, so data and information obtained previously will be used. These investigations have been based on studying the basic principles for the online and forensic monitoring of experimental of nuclear fusion reactors that generate energy from the atomic fusion of the atomic nucleus of the atom.

It also has the help of visual sensors to capture images and videos to later process and analyze them to study these different features. The first operation phase (OP1) started in 2017, and IPP offers now a large amount of the resulting data as images and videos for research.

The proposed project will develop a spatial map, that will register the 2D pixels captured by the IR cameras and the 3D structures in the fusion reactor core. For each image pixel, this will result in an estimate of the corresponding surface of the actual device element being imaged.

1.2 Requirements and specifications

The software that we are going to use for the development of the project are Python 3.8 and Matlab R2020b using a Microsoft Surface with Intel® processor Core™ i7 7660U CPU @ 2.50GHz, 64-bit operating system and 8.00 GB of RAM.

Project requirements:

- Analyze information and data extracted from previous projects.
- Concepts and basic techniques of 3D capture, analysis and representation using range sensors.
- Depth and visual data acquisition practical knowledge.
- Analysis with Point Cloud Library tools.
- Programming knowledge (Python, C++, Matlab).
- Basic knowledge requirements of image and video processing.

Project specifications:

- To explore the scene model attributes (CAD) stored in the experimental file format (.h5) used for W7-X.
- To develop a geometric strategy to estimate the surface of the corresponding element being projected for each IR image pixel.
- To design a method to validate the estimation and evaluate the error.
- To implement the strategy in the GPI repository.
- To apply it to the analysis tasks developed in previous project and collaborate with the parallel project (Thermal Image Processing for Plasma Facing Components) to measure the actual surface of the detections.

1.3 Methods and procedures

The analysis of Plasma Facing Components (PFCs) was done in previous projects by ET-SETB students. It will benefit from such a spatial map, as the detected areas of the image will now be assigned an actual surface of the device. A first attempt to explore the goal of the current proposal was also investigated with different implementation tools.

The project will start from the carried-out studies about detection and classification of thermal events on these plasma facing components, and the main goal of getting the estimation, for each image pixel, of the corresponding surface of the device element will be calculated. To do so, we will use the .h5 files obtained from the W7-X data archive to analyze the information and calculate the surface area we need.

1.4 Work Plan

This project was structured with the following work packages and Gantt diagram.

1.4.1 Work Packages

- WP 1: Theoretical concepts
- WP 2: Information analysis and research
- WP 3: Project development
- WP 4: Results and final conclusions
- WP 5: Final presentation

1.4.2 Gantt Diagram

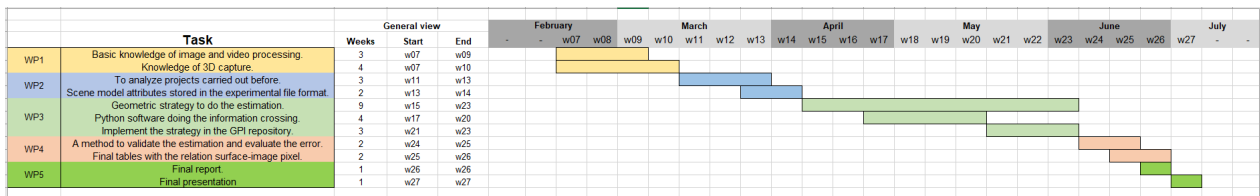


Figure 1.1: Gantt Diagram.

2 Background

This chapter explains the theoretical background that holds this project.

2.1 Introduction to nuclear fusion

Nuclear fusion consists of a reaction and particle emission in which two atomic nucleus are converted into a heavier nucleus. As in fission nuclear reactors, the objective is to extract energy from the heat produced by the nuclear reactions. This heat can be extracted from the reactor with a heat exchanger that could drive a turbine and, using an alternator, convert the initially thermal and then mechanical energy into electricity. The fuel used is deuterium, one of the stable isotopes of hydrogen, which can be obtained from seawater at a ratio of thirty grams of deuterium for each cubic meter of water.

The aim of the constant experiments based on fusion energy input is to improve these reactor prototypes, since at present more energy is spent on obtaining the fuel than is generated. Also, the aim is to obtain the necessary temperature to reach the plasma state and overcome the Coulomb barrier at atmospheric pressure (150 million degrees).

What differentiates the different types of nuclear fusion reactors that use magnetic confinement to control the plasma is the shape of the core containing the plasma. In our project we work with a type called Stellarator, which combines a poloidal and toroidal shape, namely the so-called Wendelstein 7-X. (Figure 2.1).

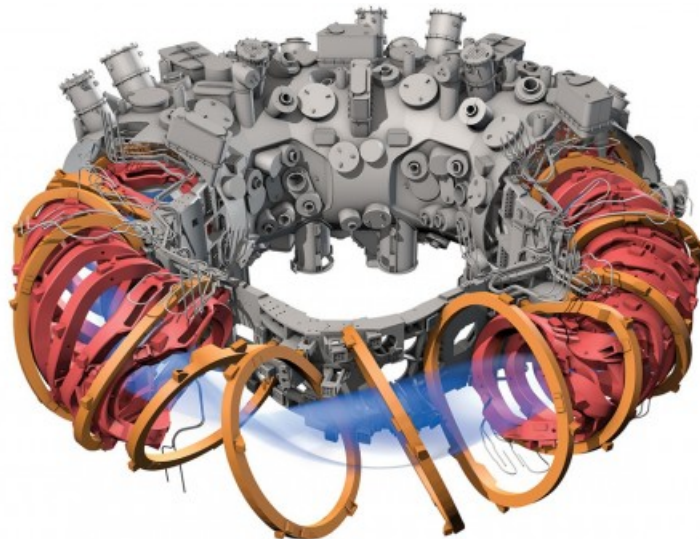


Figure 2.1: Stellarator. *Image extracted from: <https://blogthinkbig.com/alemania-quiere-cambiar-para-siempre-la-forma-en-que-consumimos-energia>.*

2.2 Wendelstein 7-x

2.2.1 Introduction to W7-X

Wendelstein 7-x is an experimental magnetic confinement nuclear fusion reactor in Greifswald, Germany. The Wendelstein 7-X device is based on a five-field Helias configuration. It is mainly a toroid, consisting of 50 non-planar and 20 planar 3.5 m high superconducting magnetic coils, which induce a magnetic field that prevents the plasma from colliding with the reactor walls. The 50 non-planar coils are used to adjust the magnetic field. They target a plasma density of 3×10^{20} particles/ m^3 , and a plasma temperature of 60-130 MK.

The experiments performed inside the reactor are based on generating plasma clouds, moving them through magnetic fields to create a contact with the heat exchangers, known as divertors, in order to extract energy from the plasma.

2.2.2 Structure of the reactor

The inner face of the fusion chamber is constituted by different parts called Plasma Facing Components (PFCs). Each of them carries specific functions:

- Divertor Targets: part of the chamber where the exchange of energy with the plasma takes place.
- Inner Wall Shield and Outer Wall Vessel: responsible for creating the chamber in order to generate the void.
- Pumping gap: Part of the chamber where impurities present in the plasma are extracted from the reactor.

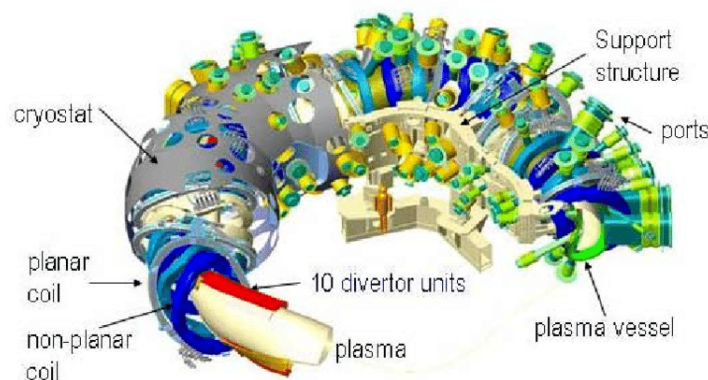


Figure 2.2: Structure of Wendelstein 7-x. Image extracted from: <https://www.researchgate.net/figure/Components-of-Wendelstein-7-X>.

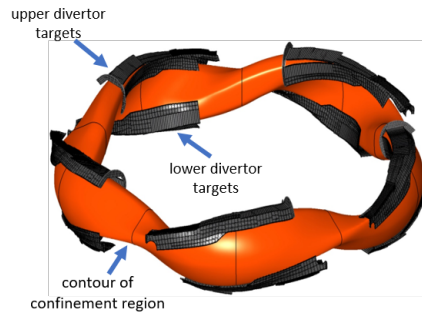


Figure 2.3: Divertor targets in Wendelstein 7-x from *PhysicsW7X*.

2.2.3 Infrared cameras

Apart from comprehending the behavior of the plasma in different configurations of the reactor, the cameras are fundamental for detecting failures like overheating.

A set of cameras operating on visible and infrared (thermal) spectrum respectively, placed in specific locations of the chamber where the plasma is travelling such that they record the flux for every experiment.

As the system is actually complex in structural terms and the cost of the construction is high at the same time, it is very important to employ these cameras to prematurely detect possible failures when the plasma is set in order to avoid irreparable damage.

In this project we have used images captured from the infrared band cameras. These cameras are distributed in such a way that each one focuses on one of the divertors of the reactor.

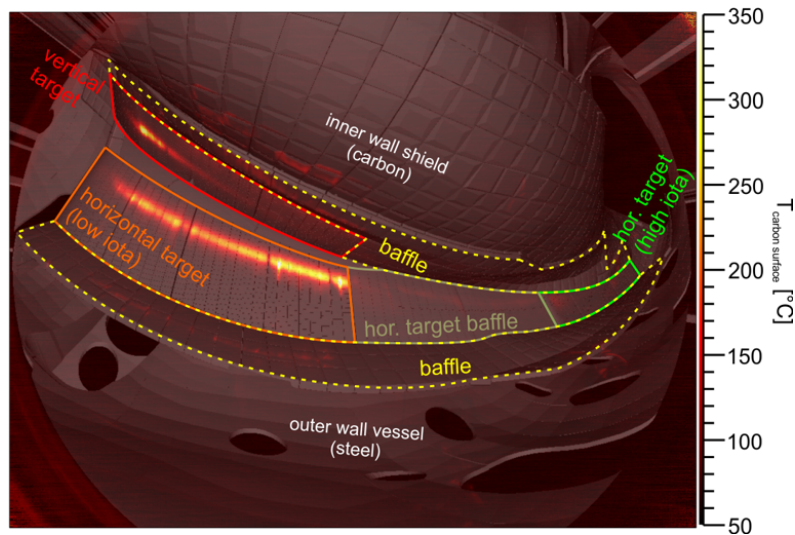


Figure 2.4: Divertor parts seen from the IR camera from *M. Jakubowski et al. (2018), Rev. Sci. Instr. 89, 10E116*.

These cameras are not positioned perpendicular to the inner walls of the reactor, so the

farthest parts of the reactor are seen under perspective and less accurate in detecting temperatures, as the surface area measured by each pixel is larger. Around the target, the detected temperatures are not accurate due to thermal noise of the sensor generated by the projection of infrared radiation, so temperature peaks can be generated in some pixels that do not correspond to the actual measurements.

2.2.4 Images in the infrared spectrum

To obtain the data from the sensors, EUROfusion and IPP use a software platform to visualize audiovisual data from the sensors and from which frames can be extracted to process each image.

These files are in HDF5 format and the extracted frames are retrieved in a two-dimensional matrix format, in which each position of the matrix corresponds to a pixel of the image.

The project will start by analyzing this extracted data to know what kind of information it contains and how we can work with this format that is generally used to store multimedia files of experiments.

3 Methodology

As we have concluded in the previous section, the project starts with a first analysis of the files that have been extracted in previous projects. These files, which are in .h5 format, are formed by different parameters that we will analyze and that later will serve us to propose the solution to find the surfaces. The geometric strategy used was based on Fabio Pisano's [4] initial proposal to calculate the area from the 3D concepts and the registration of the CAD with the respective pixels.

3.1 Scene model attributes (CAD) stored in the experimental file format (.h5) used for W7-X

3.1.1 HDF5 format

Hierarchical Data Format (HDF) is a set of file formats (HDF4, HDF5) designed to store and organize large amounts of data. HDF5 simplifies the file structure to include only two major types of object:

- Datasets, which are multidimensional arrays of a homogeneous type.
- Groups, which are container structures which can hold datasets and other groups.

3.1.2 Spatial Map

Spatial Map is a 3D reconstruction of the Scene Model of the reactor that provides the information about which each part of the reactor is seen by which pixels. It consists of images of size 768x1024 pixels. As the cameras do not move, each pixel corresponds to a specific area of the reactor. This area will be the one we must calculate as the main objective of the project.

For this, we will have as information to analyze, a series of matrices that give us for each pixel information about its position with respect to the camera.

Also, we are provided with information from an array that, for each pixel, identifies the code of the element it belongs to. Therefore, using this array that gives us the codes of the elements, we will be able to know, for all pixels, to which element and region they belong within the reactor.

3.1.3 Scene model

The scene-model contains a pixel-based segmentation of the field of view. Pixel-wise correspondence with CAD:

- CAD view: CAD rendered image (for the visual field of the camera).
- PFC ID: a code that identifies the Plasma Facing Component.
- Emissivity ε of the point's target material.
- Distance D between the camera and the point of the element seen in that pixel.
- Angle α with normal to target surface.
- 3D world coordinates: X, Y, Z .
- ϕ and θ : The values of the toroidal and poloidal angles at that point.
- LoS: Line of Sight.

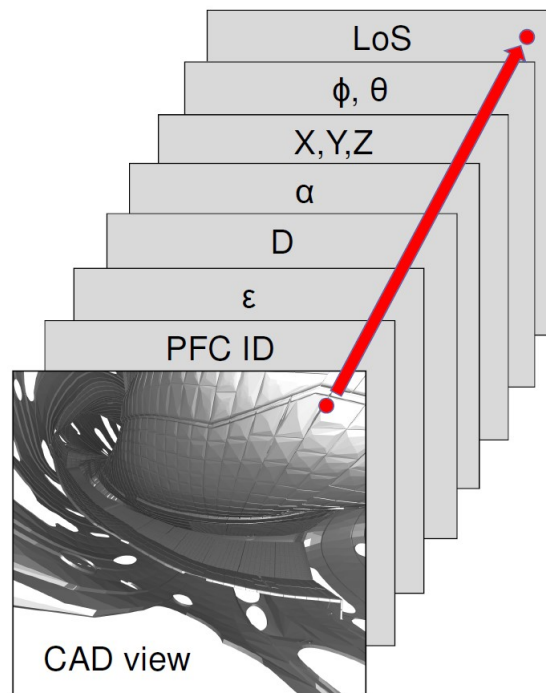


Figure 3.1: Multidimensional HDF5 image. *Image extracted from: QIR: real-time image diagnostic system for PFC protection of W7-X. A. Puig*

The spatial calibration is needed, but the problem is, given the 3D coordinates of a set of control points and their projection on the image plane, reconstruct the projection model of the camera.

3.2 Geometric strategy to estimate the surface of the corresponding element being projected for each IR image pixel

To develop a geometric strategy to estimate the surface area of the elements, we have to calculate the observed area for each pixel. That is, we have to know the intersection, which would be the contour of the region, between the field of view and the surface we are observing. To perform these calculations we have the following data:

- Camera model: The position and orientation of the camera are obtained by a calibration process. Also the distortion coefficients of the lenses and the intrinsic parameters of the camera. With this it is possible to convert the coordinates of each 3D point observed by the camera in pixel coordinates. The horizontal and vertical angle of each pixel can also be calculated.

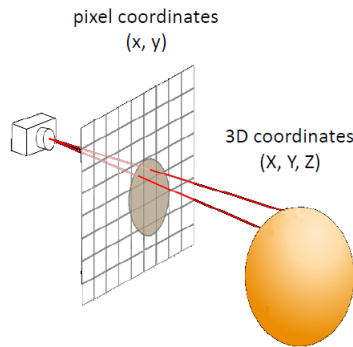


Figure 3.2: Projection from 2D coordinates to 3D coordinates . *Image extracted from: QIR: real-time image diagnostic system for PFC protection of W7-X. A. Puig*

- Scene model: As mentioned above, the Scene Model provides the 3D coordinates of the center of each pixel, the distance from the camera to the center of each pixel and the angle between the line of sight and the surface normal for each pixel center.

Within the Scene model, the data files we are interested in to create our software are the following:

- Dataset X: It is the matrix of the x-coordinate of the image.
- Dataset Y: It is the matrix of the y-coordinate of the image.
- Dataset Z: It is the matrix of the z-coordinate of the image.
- Dataset PFC: It is a matrix that relates the positions of the previous coordinates with the element of the reactor to which each pixel belongs.
- CAD files: It is the 3D design of each reactor element.

Thus, it is possible to create a program that analyzes the image of the .h5 file and calculates the area of a set of specific pixels that make up a reactor element, and then compare it with the actual area that can be obtained through the .CAD files.

From these data, which are extracted from the .h5 files available from the W7-X data archive, the method used is explained based on the following image.

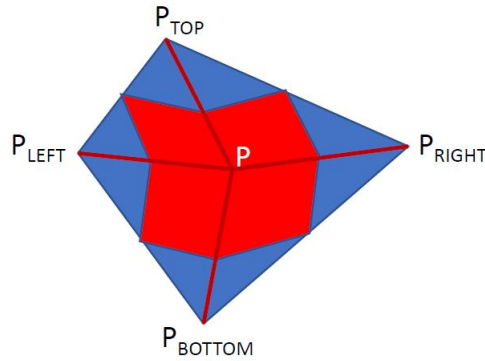


Figure 3.3: Geometric strategy to estimate the surface. *Image extracted from: Images meeting. Updates on Strike-Line Segmentation, Pixel area estimation and NN modeling. F. Pisano*

As shown above, we can assume that the visual field of a pixel P covers a 3D area bounded by the center points of the line joining the 3D position of pixel P with the 3D positions of the neighboring pixels, which are the upper neighboring pixel, bottom neighboring pixel, left neighboring pixel and right neighboring pixel.

With this, it is possible to calculate the midpoints between the neighbors obtaining four quadrilaterals that join with the central point P .

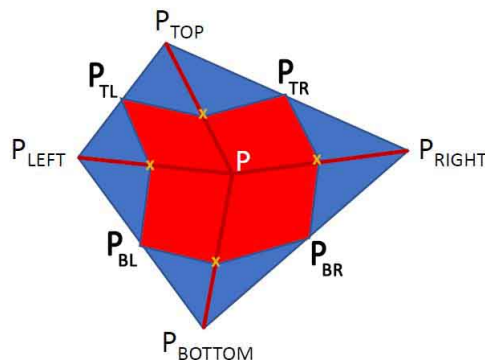


Figure 3.4: Geometric strategy to estimate the surface. *Image extracted from: Images meeting. Updates on Strike-Line Segmentation, Pixel area estimation and NN modeling. F. Pisano*

As can be seen, this strategy is valid in cases where the center of the pixel is surrounded by its four neighboring pixels, but in case of surface boundaries, where it has no neighboring pixels or the pixels are empty, it would have to be evaluated with the remaining spaces, taking the central pixel as a reference and making an approximation.

Then, the vectors that go from the central pixel to each adjacent neighboring pixel are plotted, resulting in four unit vectors. These vectors are calculated by the difference between the x, y and z coordinates of the central point and each adjacent point, obtaining four parallelograms.

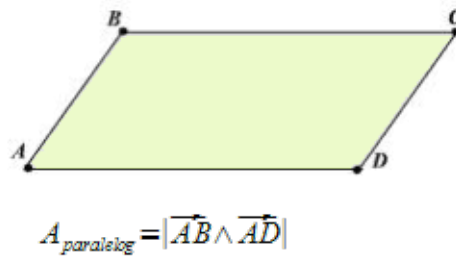


Figure 3.5: Parallelogram area

The area of each parallelogram obtained is calculated by the cross product of the vectors that form it. Finally the total area is the sum of the four areas of the forming parallelograms passed through all the pixels of the image. In the next section, it will be possible to adjust the software to repeat the process of calculating the areas of parallelograms only in the regions that is wanted. That is, as each part of the reactor corresponds to a PFC-ID, it will be possible to perform the calculation on the specific pixels that will form the part of the reactor where the area needs to be known.

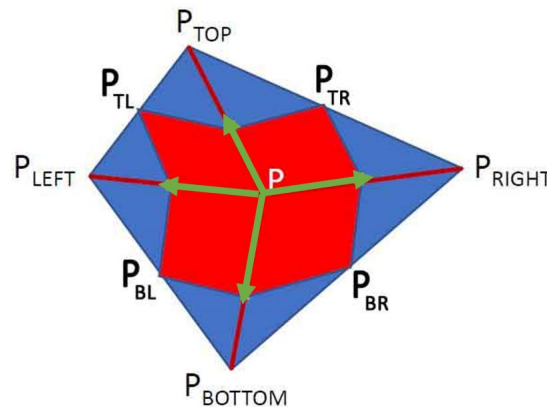


Figure 3.6: Four unit vectors that form parallelograms.

Obviously, looking at the proposed scheme, the calculation of areas would be quite simple and accurate, but there are different cases that make it difficult to calculate it.

Looking at the following figure, it is possible to see that there are cases in which if the green pixel is taken as the central pixel, its neighboring pixels may not be in the same element or even be in a void (Nan).

It is for this reason that the mirroring technique is used to refine the results because if we were to take directly the neighboring values that do not correspond to the element, the area estimation would be much more inaccurate.

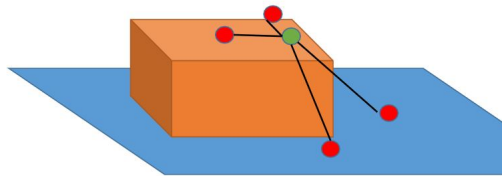


Figure 3.7: 3D illustration of the geometric strategy.

3.3 Software development to obtain the surface estimation

The program has been implemented using Matlab. The choice of this language is due to the fact that it is personally more visual to deal with the values of the matrices that form the datasets of the Scene models. The program has been divided into the following parts:

1. Opening of .h5 format files and analysis of the data. The name of the file to be opened can be modified so that it can be used with more than one file.
2. Create the conditions to find the central pixels mentioned in the previous section (without taking into account the contours).
3. First, the pixels of the region under study are searched (searched from the numerical values of the PFC-ID) and the values of the adjacent pixels are checked to ensure that they are of the same PFC-ID.
4. The unit vectors that form the x, y and z coordinates are calculated and the area of each parallelogram is calculated.
5. The process is repeated until no more values of the PFC-ID being searched for are found.
6. The program prints the sum of all these traversed areas obtaining a final value in square meters of the area of the searched region.

Step 3 is replaced by these two other experiments to see what variance of estimation error we obtain using one methodology or the other:

- Previously omitted values are taken into account, i.e. neighboring pixels whose values are empty (NaN) or that some of their neighboring pixels are not of the same value as the PFC-ID under analysis. Regardless of the PFC-ID, the values of the neighboring pixels are taken, even if they are different and are part of another element.
- Contours are still taken into account, but in this case, instead of directly taking the PFC-ID of the neighboring pixels that do not correspond to the treated element, mirroring is performed in these cases. That is, if a neighboring pixel has a different PFC-ID, the value of this one is taken to match the reactor element.

3.4 Method to validate the estimation and error evaluation

In order to know if the surface area calculated by the geometrical strategy used in the previous section corresponds to the real surface area of the reactor elements, CAD files have been provided. These CAD files are in .stl format and the ABViewer program has been used to visualize them. Using this program it is possible to measure the surface of the elements we are studying, since each element of the reactor corresponds to a CAD file.

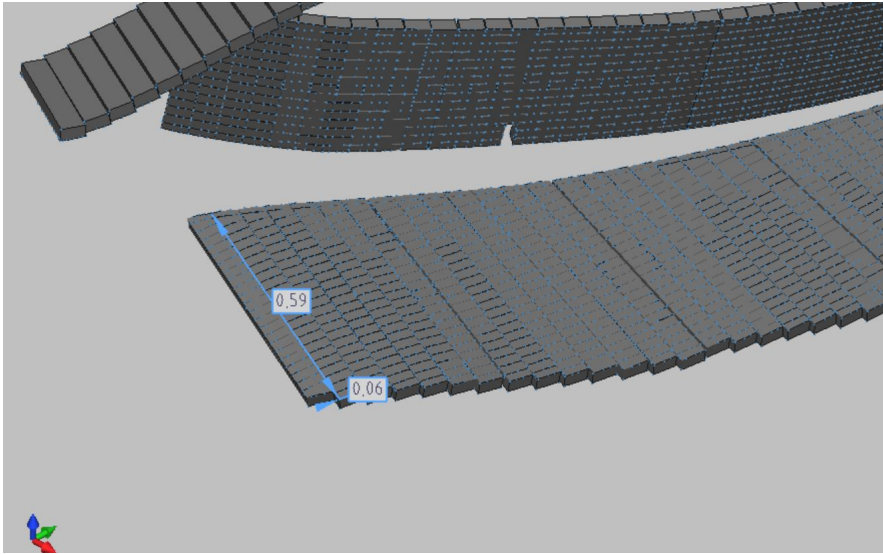


Figure 3.8: CAD file opened by ABViewer. Measurements to calculate the surface area.

To know which .h5 file is being treated, we also have access to the PFC ID hierarchy that is used to analyze the IDs of the files and to know which element corresponds to that file. Therefore, knowing with this PFC-ID table which element the .h5 file corresponds to, it is possible to validate the estimation made with it by comparing the surface obtained with the program with the one measured by ABViewer.

4 Results and statistics

In this chapter, the main parts of the experimental work are explained in detail.

4.1 Estimation of the surface of the corresponding element being projected for each IR image pixel

The program calculates the sum of areas formed by the pixels of each region of the reactor parts. The PFC-ID of the divertor fingers, which are the smallest elements forming the regions, are used for the calculation accuracy.

The PFC coding is hierarchical, and it can be better described by looking at the PFC ID's as strings of bit. Each PFC ID is a 32 bits number. The first 4 bits define the CAD component. The next 3 bit defines the part of the CAD component and the next 2 bits define the module of the part. The other 4 bits define the finger and the next 19 bits define the connected component as we can see in the following table:

PFC ID (first 13 bits)	#	COMPONENT	PART	MODULE	FINGER	
0000000000000	0	N/D				
0001000000000	512	Void				
0010000000000	1024	Baffle	Horizontal Target			
0010001000000	1088		Vertical Target			
0011000000000	1536	Closure				
01000000 0000-0110	2048-2054	Divertor	Low Iota Target	TM1h	0-6	
01000001 0000-0110	2064-2070			TM2h	0-6	
01000010 0000-0111	2080-2087			TM3h	0-7	
01000011 0000-0111	2096-2103			TM4h	0-7	
01000100 0000-1011	2112-2123		Middle Target	TM5h	0-11	
01000101 0000-1011	2128-2139		TM6h	0-11		
010001000 0000-0101	2176-2181		High Iota Target	TM7h	0-5	
010001001 0000-1011	2192-2203			TM8h	0-11	
010001010 0000-1011	2208-2219			TM9h	0-11	
010001100 0000-1001	2240-2249		Vertical Target	TM1v	0-9	
010001101 0000-1001	2256-2265			TM2v	0-9	
010001110 0000-1000	2272-2280			TM3v	0-8	
0101000000000	2560		Panel			
0110000000000	3072		Pumping gap			
011100000 0000-0101	3584-3589		Scraper			0-5
1000000000000	4096	Shield				
1001000000000	4608	Immersion Tube				
1010000000000	5120	Langmuir Probe				
1011000000000	5632	Limiter				

Figure 4.1: PFC ID.

In this case, it is discriminated to the finger level taking the first 13 bits, just dividing the PFC ID by 2^{19} .

To validate the estimation provided by our program, the measurements of the surfaces are made with the CAD files, to obtain the real area of each part of the divertor.

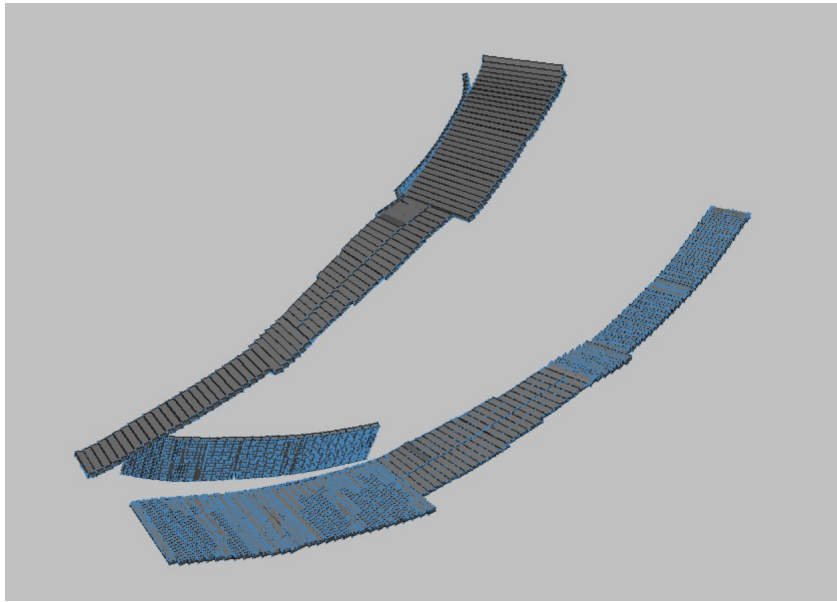


Figure 4.2: Divertor .CAD file.

The most important thing here is to know how to orient the elements of the .CAD files in order to correctly identify the parts of the divertor.

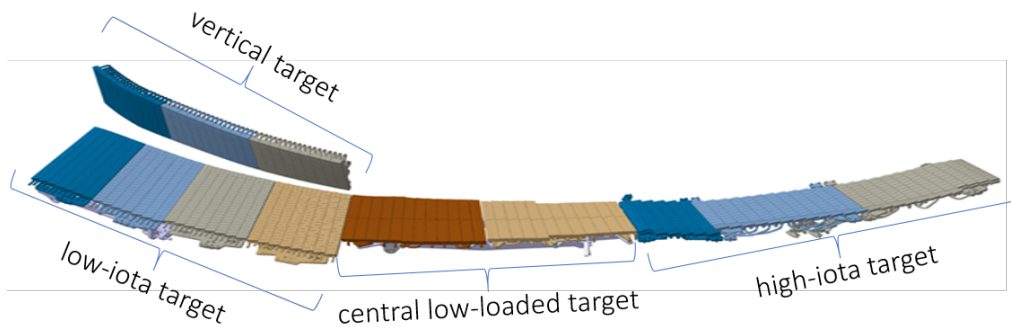


Figure 4.3: Divertor parts identification.

The results obtained are compared by means of the PFC-ID, which indicates the set of pixels that form each part. Thus, by comparing the result obtained with the program indicating which PFC-ID is being measured, looking at the measurement made with ABViewer, it is possible to calculate the percentage of error made by the program.

4.2 Results

The summary of the procedure is as follows and the results obtained with the most important parts of the divertor are discussed below.

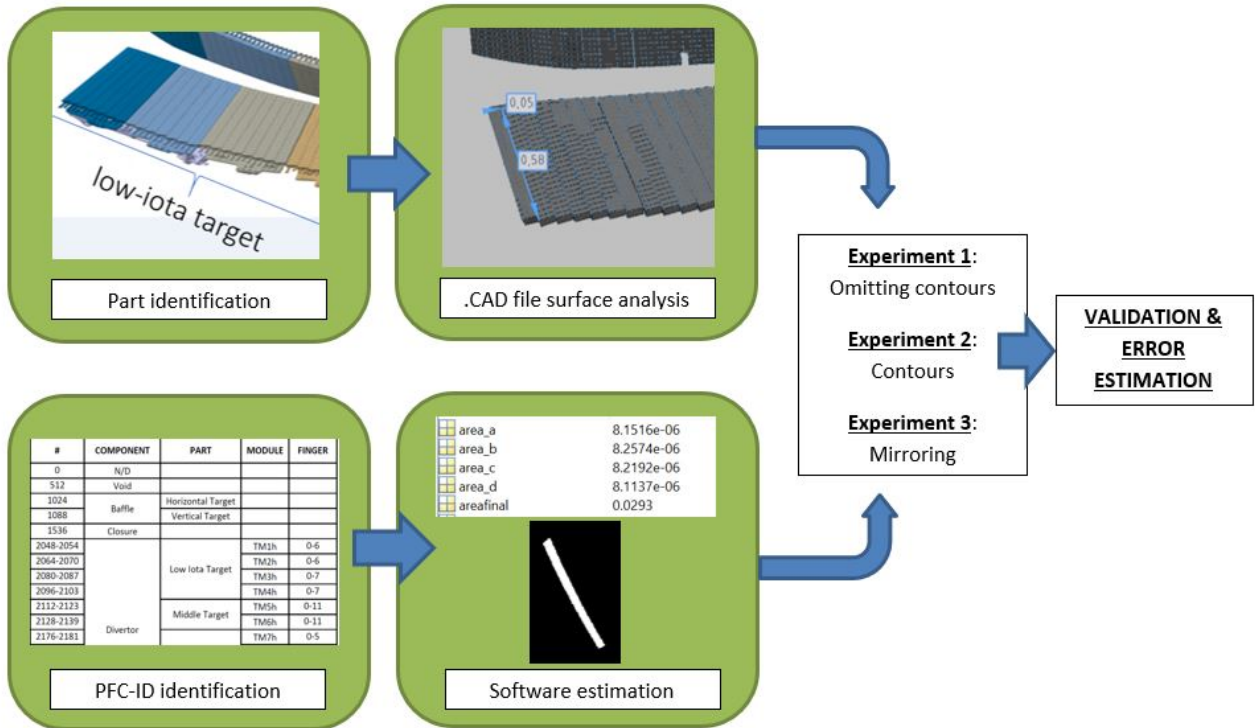


Figure 4.4: Process diagram.

- Experiment 1: A first study of the results was carried out without taking into account the contours of the parts to be analyzed. That is, the program calculated the area formed only with the pixels that coincided with the PFC-ID (both the central pixel and its four neighbors).
- Experiment 2: The second experiment that has been performed has been taking into account the neighboring pixels with the PFC-ID values that correspond to them, that is, taking into account the contours by taking the values, even if they are not part of the same element. Unlike the first experiment in which the contour values were omitted because they contained neighboring pixels of different PFC-ID, in this case it can be seen that the estimated error is better, since the contours have been taken into account instead of omitting them.
- Experiment 3: As it has been seen that the result taking into account the contours is better, it has been looked for a way to improve this error estimation and it has

considered mirroring these conflicting neighboring pixels. That is, instead of taking the values of different neighboring pixels of the PFC-ID even if they belong to another element, mirroring these pixels so that they are part of the element. This has been done in cases where the central pixel had the PFC-ID as a value, but one or more of its neighboring pixels did not. Looking at the results it can be seen that the contours have been taken more accurately using this technique and consequently the estimation error has been lower.

Let's see all the cases in tabular format to facilitate visual comprehension.

CAD: component 165 divertor m1				
PFC-ID	Module	Real Surface	Estimation	Error
2049	TM1h (2nd finger)	$0.0295m^2$	$0.0263m^2$	10.84%

Table 4.1: Exp. 1: Low Iota Target. Omitting contours.

CAD: component 165 divertor m1				
PFC-ID	Module	Real Surface	Estimation	Error
2049	TM1h (2nd finger)	$0.0295m^2$	$0.0317m^2$	7.45%

Table 4.2: Exp. 2: Low Iota Target. Contours.

CAD: component 165 divertor m1				
PFC-ID	Module	Real Surface	Estimation	Error
2049	TM1h (2nd finger)	$0.0295m^2$	$0.0293m^2$	0.6779%

Table 4.3: Exp. 3: Low Iota Target. Mirroring.

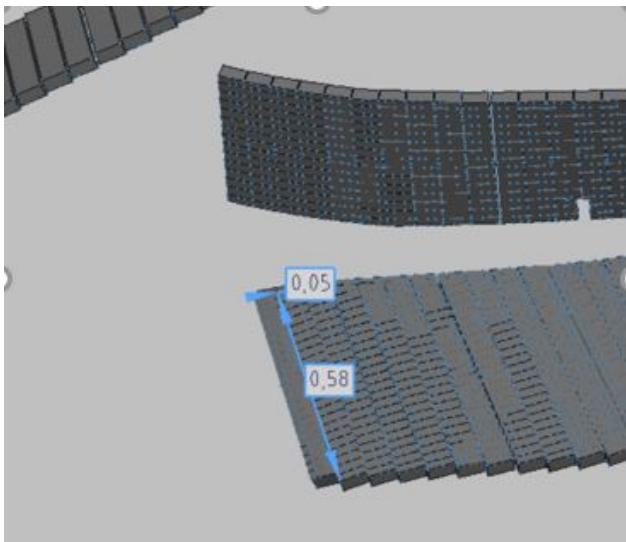


Figure 4.5: Low Iota Target. Surface measurement: 0.58m x 0.05m.

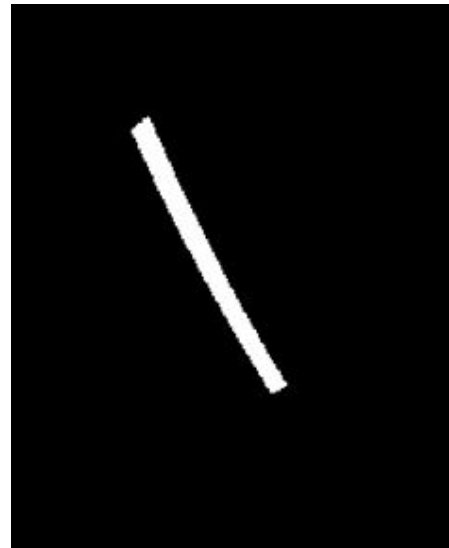


Figure 4.6: Low Iota Target. Surface estimation mask.

If the results are observed, an underestimation can be seen in the case of omitting the contours, where the error is 10.84%, but in the case of taking into account the contours this error decreases considerably until having a very low estimation error in the case of mirroring. Also, being an element that is close to the point of view, the accuracy of the estimation is better. ya que en está posición según la línea de visión cada píxel corresponde a una área más pequeña, en este caso, el finger analizado está formado por 1028 píxeles y la superficie por píxel es de $2.8502e-05m^2$.

CAD: component 165 divertor m1				
PFC-ID	Module	Real Surface	Estimation	Error
2112	TM5h	$0.0132m^2$	$0.0117m^2$	11.36%

Table 4.4: Exp. 1: Middle Target. Omitting contours.

CAD: component 165 divertor m1				
PFC-ID	Module	Real Surface	Estimation	Error
2112	TM5h	$0.0132m^2$	$0.0142m^2$	7.57%

Table 4.5: Exp. 2: Middle Target. Contours.

CAD: component 165 divertor m1				
PFC-ID	Module	Real Surface	Estimation	Error
2112	TM5h	$0.0132m^2$	$0.0130m^2$	1.51%

Table 4.6: Exp. 3: Middle Target. Mirroring.

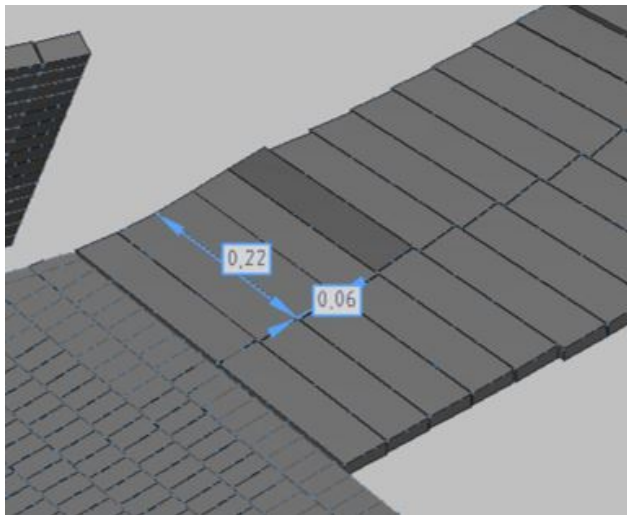


Figure 4.7: Middle Target. Surface measurement: 0.22m x 0.06m.

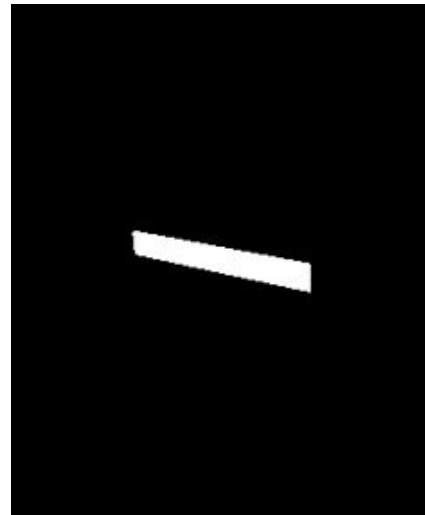


Figure 4.8: Middle Target. Surface estimation mask.

CAD: component 165 divertor m1				
PFC-ID	Module	Real Surface	Estimation	Error
2128	TM6h	$0.0095m^2$	$0.0090m^2$	5.26%

Table 4.7: Exp. 1: Middle Target. Omitting contours.

CAD: component 165 divertor m1				
PFC-ID	Module	Real Surface	Estimation	Error
2128	TM6h	$0.0095m^2$	$0.0099m^2$	4.21%

Table 4.8: Exp. 2: Middle Target. Contours.

CAD: component 165 divertor m1				
PFC-ID	Module	Real Surface	Estimation	Error
2128	TM6h	$0.0095m^2$	$0.0094m^2$	1.05%

Table 4.9: Exp. 3: Middle Target. Mirroring.

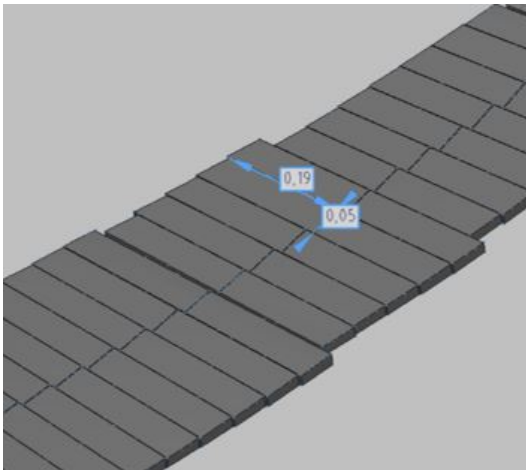


Figure 4.9: Middle Target. Surface measurement: 0.19m x 0.05m.

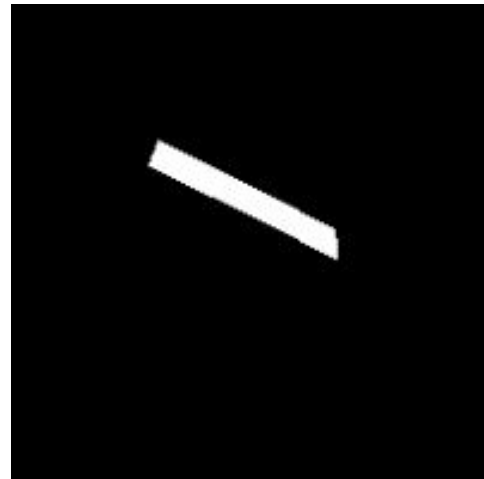


Figure 4.10: Middle Target. Surface estimation mask.

In this case, also as in the low iota, the element is in a plane perpendicular to the line of sight and each pixel corresponds to an area of $2.0785e-05m^2$. This makes the estimation error considerably low in case of mirroring.

CAD: component 165 divertor m1				
PFC-ID	Module	Real Surface	Estimation	Error
2245	TM1v	$0.018m^2$	$0.0213m^2$	18.33%

Table 4.10: Exp. 1: Vertical target. Omitting contours.

CAD: component 165 divertor m1				
PFC-ID	Module	Real Surface	Estimation	Error
2245	TM1v	$0.018m^2$	$0.0198m^2$	10%

Table 4.11: Exp. 2: Vertical Target. Contours.

CAD: component 165 divertor m1				
PFC-ID	Module	Real Surface	Estimation	Error
2245	TM1v	$0.018m^2$	$0.0189m^2$	5%

Table 4.12: Exp. 3: Vertical Target. Mirroring.

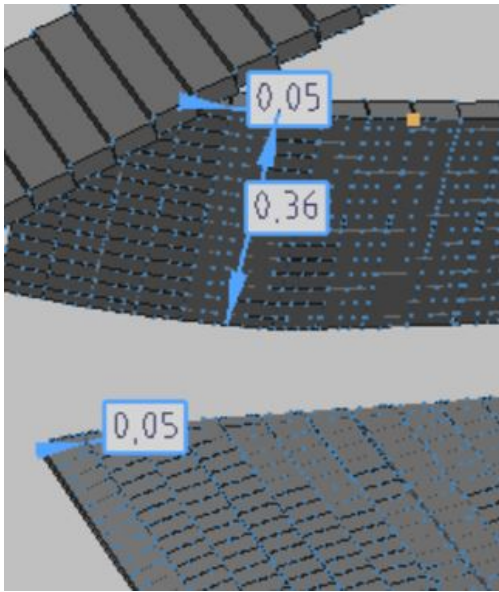


Figure 4.11: Vertical Target. Surface measurement: 0.36m x 0.05m.

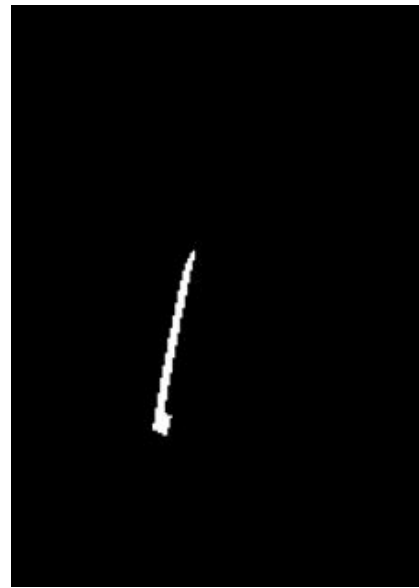


Figure 4.12: Vertical Target. Surface estimation mask.

This case is considered a special case, in which the vertical target is located practically parallel to the line of sight, which causes the area of its pixels to be larger and this makes the camera see surface points in depth perspective. This is reflected in the results, where a higher estimation error is obtained than in the previous cases. In this case, the finger being analyzed consists of 346 pixels and the average area per pixel is much higher than in the previous cases: $6.1561e-05m^2$.

CAD: component 165 divertor m1				
PFC-ID	Module	Real Surface	Estimation	Error
2192	TM8h	$0.015m^2$	$0.0114m^2$	24%

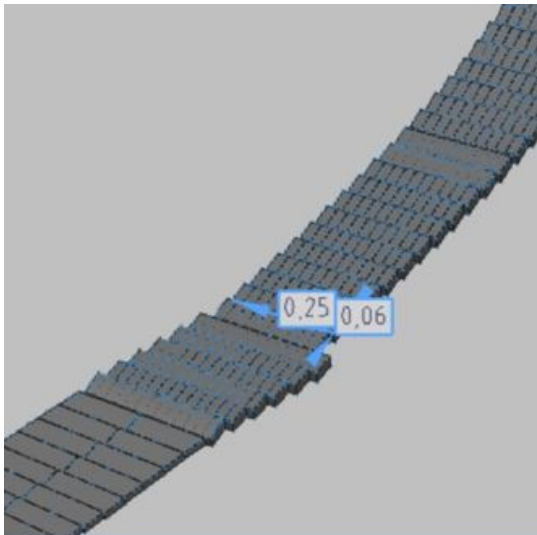
Table 4.13: Exp. 1: Higher Iota Target. Omitting contours.

CAD: component 165 divertor m1				
PFC-ID	Module	Real Surface	Estimation	Error
2192	TM8h	$0.015m^2$	$0.0172m^2$	14.67%

Table 4.14: Exp. 2: Higher Iota Target. Contours.

CAD: component 165 divertor m1				
PFC-ID	Module	Real Surface	Estimation	Error
2192	TM8h	$0.015m^2$	$0.014m^2$	6.67%

Table 4.15: Exp. 3: Higher Iota Target. Mirroring.

Figure 4.13: Higher Iota Target.
Surface: 0.25m x 0.06m.Figure 4.14: Higher Iota Target.
Surface estimation mask.

It can be observed in the results that in the Higher Iota the estimation error is the highest. This is because it is the part of the divertor that is farthest away from the observation point in the image. This makes the pixel area bigger ($6.7961e-05m^2$) and the calculation of the area more inaccurate. This is also reflected in the number of pixels that form this part of the reactor, the farther away it is from the observation point of the image, the less pixels (205) form the element and therefore the less precision of calculation. This could be improved by placing another camera in a better position to capture this part of the divertor or by taking a higher resolution camera to better capture the far pixels.

4.3 Project real application

These area estimations can help other research projects in the field of Wendelstein 7-X. At the end of this project it has been possible to apply the results obtained by collaborating with David Vizcarro's project in order to improve the results of each other's reports.

To this end, David has been provided with the estimates of areas per pixel of all the Scene Models. This is a matrix of the sensor image size, where each element of the matrix is the pixel where the area estimate obtained with the geometric strategy of the neighboring pixels from the XYZ coordinates is stored. With this area estimation per pixel, it is possible to obtain the approximate real surface of the masks that David obtained from the hotspots and strike lines detector.

To summarize, David's project takes a sequence of reactor states in which all object appearances can be observed. To be more precise, it is possible to see the different related components in a graph that he creates, i.e. all the detections in a thermal event during the consecutive frames of the sequence.

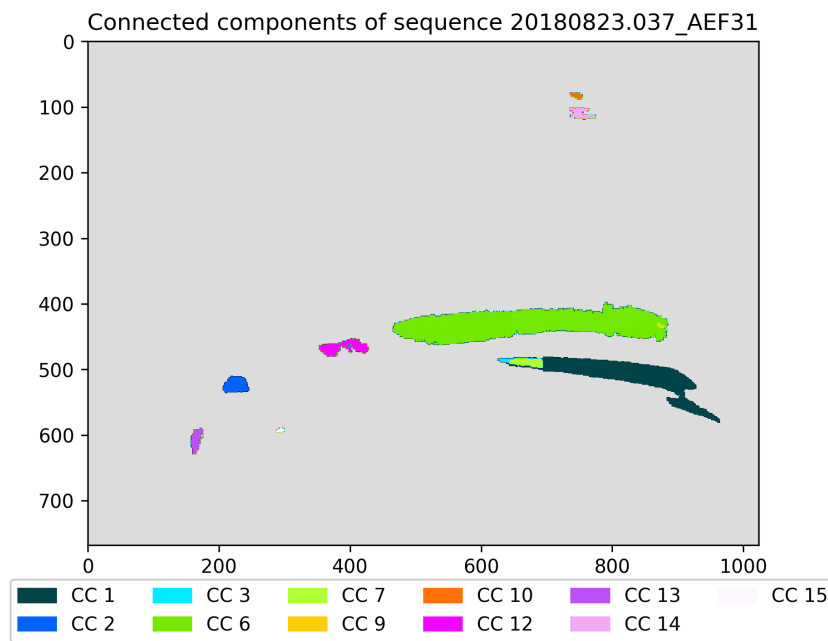


Figure 4.15: Object appearances.

With this, the following graphs are obtained. These graphs refer to the evolution of the measurement of each of the previous related components. The first one makes the calculation with the total pixels of a region and the second one takes advantage of the current project to use the area matrices of each pixel, where multiplying each pixel of the related component by the matrix, we obtain the sum of the total area.

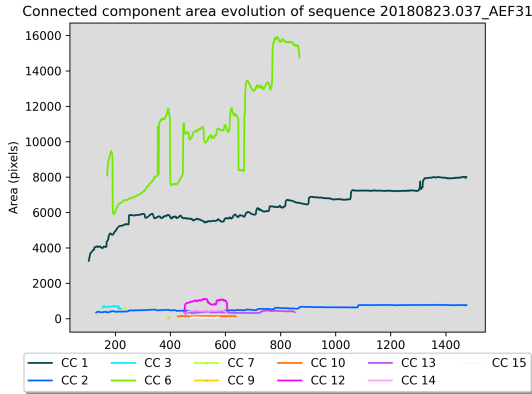


Figure 4.16: Connected component area evolution in pixels.

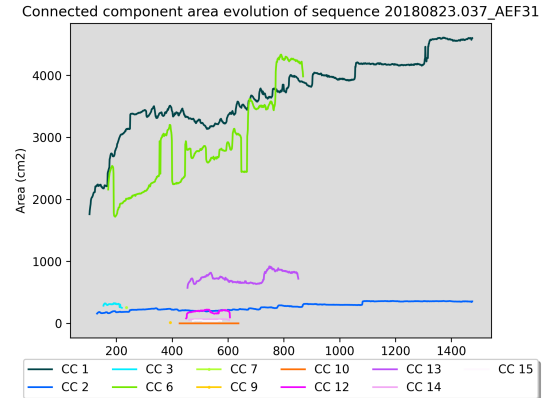


Figure 4.17: Connected component area evolution in cm^2 .

Thus, thanks to the area estimation, visual results can be obtained. The areas in pixels, which is the one on the left, and in square centimeters, which is the one on the right, it is possible to see how the connected component in the lower left margin of the first image (CC1) has a different evolution of the areas in the two images, as it is smaller in total pixels than the light green region (CC6). This is when it is observed thanks to the help of area estimation that this is caused by the camera perspective, so CC1 has a physical area larger than the apparent area in pixels. Something similar happens with the lilac connected component (CC13).

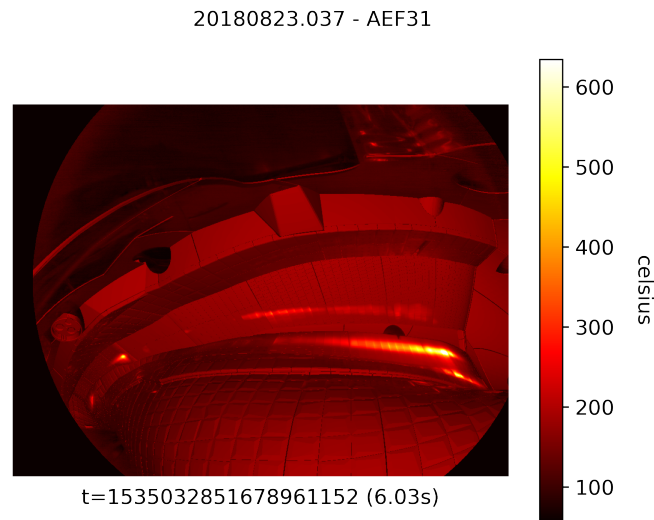


Figure 4.18: 20180823.037 AEF31 frame.

Also, it can be seen in the two strikelines that occur in the horizontal target, CC6 in the previous plots, and in the vertical target which is CC1. Although the region CC1 seen in the vertical target strikeline is smaller in pixels, its pixels have a larger area. This is because it is located in the plane of the vertical target, which is very parallel to the line of sight, so the camera sees the surface points in depth perspective. On the other hand, the surface points of the CC1 region of the horizontal target are in a plane almost perpendicular to the line of sight and each pixel corresponds to a smaller area.

5 Conclusions and Further Research

After obtaining the results of three types of experiments to improve the program, it can be concluded that the main objective of the project has been achieved. Consistent results have been obtained that have allowed to be applied directly to another parallel project.

At the beginning the software was started using Python, but personally, having to make use of datasets and matrices of quite large sizes, it has been preferred to continue with Matlab in order to better illustrate the results. This has allowed us to have a more illustrative view of the pixels and the elements to be taken into account in order to better understand the geometrical strategy of the calculation of the areas per pixel.

As first results were obtained quite important estimation errors that could be corrected thanks to suggestions and analysis carried out with the project tutor. After different meetings and improvement proposals, more acceptable results have been obtained in which, as we have said, depending on the elements that are near or far from the line of sight, the estimation error increases or decreases.

It has also been commented that with better resolution cameras, much more accurate results could be obtained by having more pixels to estimate the areas or even if other cameras were added to capture other points of view, these inaccuracies of the elements farther away from the focus of the current camera could be corrected.

On the other hand, I would like to mention the pleasure of being able to attend meetings of the EUROfusion group that are currently working on projects related to Wendelstein 7-X and the feeling of having been able to contribute to this research is very satisfactory. As future improvements we could think of geometric strategies that can calculate the areas per pixel of irregular surfaces and be able to apply the estimation of areas in all parts of the reactor.

After finishing the project the sensations are positive after having been able to reach a geometric strategy to solve the problem initially posed, to have obtained first results that with different experiments and new strategies have been improved and finally to value the work done after seeing that it has been able to be used in other projects in a satisfactory way.

6 Bibliography

- [1] Aina Palacios. Anomalies detection in the infrared spectrum of Plasma Physics at Wendelstein 7-X. June, 2019.
- [2] B. Cannas, A. Fanni, F. Pisano, G. Sias. Images meeting. Updates on Strike-Line Segmentation, Pixel area estimation and NN modeling. January 2019.
- [3] F. Pisano, B. Cannas, M. Jakubowski, H. Niemann, A. Puig Sitjes, and G. Wurden. Towards a New Image Processing System at Wendelstein 7-X: From Spatial Calibration to Characterization of Thermal Events. *The Review of scientific instruments*, 2018.
- [4] F. Pisano et al., “Tools for Image Analysis and First Wall Protection at W7-X,” presented at the 3rd IAEA Technical Meeting on Fusion Data Processing, Validation and Analysis, Vienna, 2019. [Online]. Available: <http://hdl.handle.net/21.11116/0000-0004-5DC0-B>
- [5] V. Moncada, THERMAVIP V 31 10 17.” [Online]. <http://cadarache.cea.fr/cad/Documents/Entreprises/Valorisation/Rencontres-CEA-Industrie/11eme/Fiche marketing THERMAVIP V 31 10 17.pdf>
- [6] Alex Puig Sitjes. QIR: rea-time image diagnostic system for PFC protection of W7-X. 2019.
- [7] IPP. Wendelstein 7-X fusion device. Max-Planck-Institut für Plasmaphysik Garching · Greifswald.
- [8] EUROfusion, “EUROfusion web site.” <https://www.euro-fusion.org>
- [9] A. Moreno Punzano. Thermal Anomalies Detection in the Infrared Spectrum at Wendelstein 7-X. Feb 2020.
- [10] A. Palacios, ”Detection, tracking and classification of thermal events on Plasma Facing Components,” Report Introduction to Research, ETSETB-UPC, June 2019.
- [11] D. Clery, “The new shape of fusion,” *Science*, vol. 348, no. 6237, pp. 854–856, May 2015, doi: 10.1126/science.348.6237.854.
- [12] D. Clery, “The bizarre reactor that might save nuclear fusion,” *Science — AAAS*, Oct. 21, 2015. <https://www.sciencemag.org/news/2015/10/bizarre-reactor-might-save-nuclear-fusion>.